PROTEINS: Structure, Function, and Genetics 33:107–118 (1998)

Folding Mechanism of Three Structurally Similar β-Sheet Proteins

Lora L. Burns, Paula M. Dalessio, and Ira J. Ropson*
Department of Biochemistry and Molecular Biology, Pennsylvania State University, College of Medicine, Hershey, Pennsylvania

ABSTRACT **The folding mechanism of cellular retinoic acid binding protein I (CRABP I), cellular retinol binding protein II (CRBP II), and intestinal fatty acid binding protein (IFABP) were investigated to determine if proteins with similar native structures have similar folding mechanisms. These mostly β-sheet proteins have very similar structures, despite having as little as 33% sequence similarity. The reversible urea denaturation of these proteins was characterized at equilibrium by circular dichroism and fluorescence. The data were best fit by a two-state model for each of these proteins, suggesting that no significant population of folding intermediates were present at equilibrium. The native states were of similar stability with free energies (linearly extrapolated to 0 M urea, ΔG_{H_2O}) of 6.5, 8.3, and 5.5 kcal/mole for CRABP I, CRBP II, and IFABP, respectively. The kinetics of the folding and unfolding processes for these proteins was monitored by stopped-flow CD and fluorescence. Intermediates were observed during both the folding and unfolding of all of these proteins. However, the overall rates of folding and unfolding differed by nearly three orders of magnitude. Further, the spectroscopic properties of the intermediate states were different for each protein, suggesting that different amounts of secondary and/or tertiary structure were associated with each intermediate state for each protein. These data show that the folding path for proteins in the same structural family can be quite different, and provide evidence for different folding landscapes for these sequences. Proteins 33:107–118, 1998.**

Key words: protein folding; folding intermediates; β-sheet proteins; structural homology; stopped flow kinetics

INTRODUCTION

Understanding how the primary amino acid sequence of a protein encodes not only the final structure, but also the means by which that structure is achieved, remains one of the major unsolved questions of biochemistry.[1–4] Although most proteins appear to follow a two-state model for folding at equilibrium, many of these same proteins show complicated folding kinetics. The classical explanation for this contradiction requires the presence of defined intermediates on the folding pathway.[5] Recently, new models for the folding process involving energy landscapes have been described.[1] In these models, there are many different possible routes from a large number of unfolded conformations to the single native state conformation. Some of these routes lead to the formation of structures that must be completely or partially unfolded before the native structure can be achieved, thus causing the complex kinetics observed during the folding of many proteins. For both the classical and new models of protein folding, an understanding of the structures and stabilities of the observed intermediate states will be crucial to understanding the folding process.

These models can be examined experimentally by comparing the folding mechanism of structurally homologous proteins. The classical model for protein folding predicts that the mechanism of folding should be conserved, since the folding path to the native state passes through unique structural states. In order to obtain the same final structure, the structure of the intermediates must also be conserved. On the other hand, the folding funnel model predicts that related proteins could follow different paths to the same final structure. This paper examines the folding mechanism of three proteins in the intracellular lipid binding protein (iLBP) family.

The iLBPs are small (14–16 kDa, 127–136 amino acids), mostly β-sheet proteins which bind various hydrophobic ligands.[6,7] The proteins consist of two five-stranded, antiparallel, orthogonal β-sheets which form an enclosed cavity for ligand binding[6] (Fig. 1). The mouth of this "β-clam" structure is closed by two short α-helices. This solvent-filled cavity is unusual in that it is lined with both polar and nonpolar amino acids and has minimal connections to external solvent. The hydrophobic core of these proteins is

Grant sponsor: National Science Foundation; Grant number: MCB 94-05282.
*Correspondence to: Ira J. Ropson, Department of Biochemistry and Molecular Biology, The Pennsylvania State University, College of Medicine, Hershey, PA 17033. E-mail: iropson@psu.edu
Received 27 January 1998; Accepted 1 June 1998

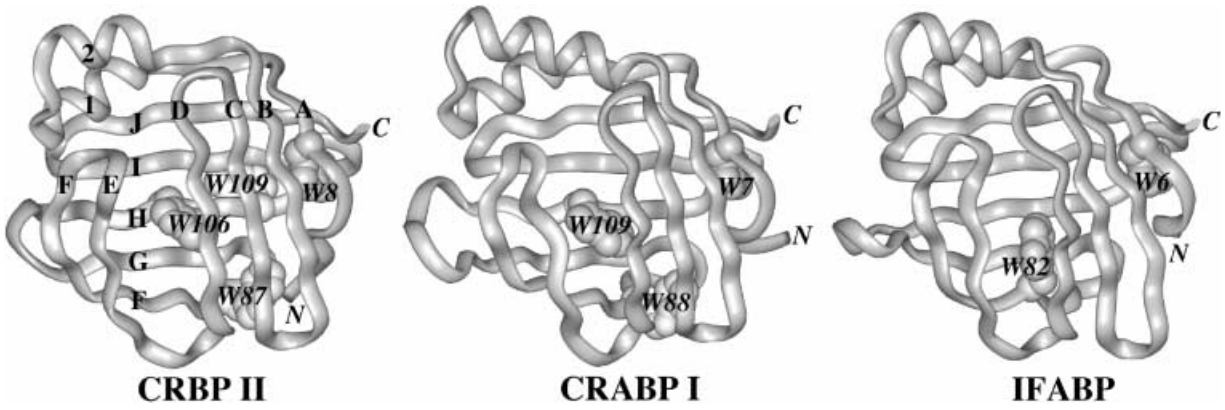

Fig. 1. Ribbon diagrams of CRBP II (A form),[56] CRABP I (B form),[57] and IFABP,[58] illustrating the structural homology and the location and orientation of the tryptophan residues. β-strands on CRBP II are labelled A–J, beginning with the N-terminal strand.

unusually small for proteins of this size and is located opposite to the two α-helices. In addition, an arc of hydrophobic residues line the perimeter of the β-sheets, holding the edges of the β-clam closed.[6]

Previous work has focused on the folding mechanism of one member of this family: intestinal fatty acid-binding protein (IFABP).[8–16] A few studies on the folding mechanism of another member of this family, cellular retinoic acid-binding protein I (CRABP I), have also been reported,[17–19] but little is known about the kinetic mechanism for unfolding of this protein. This study compares the folding and unfolding mechanisms of CRABP I and cellular retinol binding protein II (CRBP II) with that of IFABP to begin to address whether proteins with the same global fold follow the same folding pathway.

METHODS

Protein Source and Purification

E. coli expression vectors for rat IFABP,[20] mouse CRABP I,[21] and CRBP II[22] have been previously described. IFABP, CRABP I, and CRBP II were purified using a modified protocol of Sacchettini et al.[20] The supernatant of a 60% ammonium sulfate fractionation was dialyzed against 20 mM KPO_4, 1 mM EDTA at pH 7.3. The dialysate was loaded onto a Q Sepharose Fast Flow (Pharmacia) anion exchange column equilibrated with 20 mM KPO_4, 1 mM EDTA at pH 7.3 for IFABP and CRABP I. The column was equilibrated with 20 mM Tris, 50 mM NaCl, 1 mM EDTA, pH 8.0 for the purification of CRBP II. The eluent was concentrated to 50–100 ml using an Amicon ultra filtration device with a YM3 membrane and resolved over a G-50 Sephadex (Pharmacia) column equilibrated with 50 mM KPO_4, 100 mM KCl, 5 mM NaN_3 at pH 7.2. The pure protein fractions were pooled and delipidated as previously described.[23] For CRABP I and CRBP II, 0.1 mM DTT was added to all buffers prior to use. Protein purity was demonstrated by the presence of a single band on a 20% SDS polyacrylamide gel. Extinction coefficients at 280 nm were calculated by the method of Pace et al.[24]—IFABP, 16,960 M^{-1} cm^{-1}; CRABP I, 20,970 M^{-1} cm^{-1}; CRBP II, 26,470 M^{-1} cm^{-1}.

Reagents

Denaturant stock solutions (10 M urea) used in unfolding and refolding experiments were prepared as previously described.[15] Working urea solutions (9 M) were made from the 10-M stock on the day of the experiment by adding 25 mM $NaPO_4$, 75 mM NaCl, 0.1 mM EDTA at pH 8.0. The urea concentration was determined by refractive index measurements using a Milton Roy Abbe-3C refractometer at 25°C in conjunction with an equation-relating refractive index to concentration.[25] All experimental buffers contained 25 mM $NaPO_4$, 75 mM NaCl, 0.1 mM EDTA, pH 8.0. For CRABP I and CRBP II, 0.1 mM DTT was also included. Buffers were filtered through 0.2 μm Whatman nylon membranes before use. Unless otherwise noted, all chemicals were reagent grade.

Equilibrium Analysis

The total accessible surface area was calculated for the native state using the analytical surface area program (ASC) of Eisenhaber and Argos.[26] The surface area of the denatured state was calculated using the values for each amino acid in the tripeptide Gly-X-Gly.[26] The surface area in the native state was subtracted from that in the unfolded state to give the change in accessible surface area (ΔASA).

Equilibrium unfolding and refolding transitions were monitored by far-UV circular dichroism (CD), and intrinsic tryptophan fluorescence as a function of denaturant concentration. A Jasco J-710 spectropolarimeter was used to follow the spectral changes in the far-UV (250–212 nm) using a thermostatted 0.1-cm pathlength cell. Mean residue ellipticities (MRE) were calculated for the native and denatured

CD spectra using the following equation:

$$[\theta]_{MRE} = ([\theta]_{OBS} * MW)/(10 * c * 1 * n) \quad (1)$$

where c is the concentration in g/ml, 1 is the pathlength in cm, n is the number of amino acids in the protein, MW is the molecular weight of the protein, and θ_{OBS} is the ellipticity in degrees.

Fluorescent changes were followed with an Aminco–Bowman Series 2 luminescence spectrometer with excitation at 290 nm (2 nm bandpass) and emission spectra collected from 300–400 nm (8 nm bandpass) using a thermostatted 1-cm pathlength cell. All measurements were made at 25°C after sufficient time for equilibration, as determined by the lack of any further signal change. Both CRABP I and CRBP II were equilibrated 1 hour prior to obtaining equilibrium data. IFABP was equilibrated for at least 30 minutes. Protein concentrations for CD and fluorescence experiments were 7 and 0.7 μM, respectively. Reversibility of folding was demonstrated by coincident curves for native protein and protein previously unfolded in 8 M urea. All fits were to duplicate data sets for each spectroscopic method.

Nonlinear least-square fits to the equilibrium data were generated with KaleidaGraph (Synergy Software) using the following equation (2):[27]

$$X_{[D]} = \frac{(X_N + m_N[D]) + \left\{X_U + m_U[D]\exp\left(\left\{-\Delta G_{H_2O} + m_G[D]\right\}/RT\right)\right\}}{1 + \exp\left(\left\{-\Delta G_{H_2O} + m_G[D]\right\}/RT\right)}$$

where [D] is the denaturant concentration, $X_{[D]}$ is the value of the spectroscopic property at that denaturant concentration, X_N and X_U are the values for the spectroscopic property linearly extrapolated to [D] = 0 for the native and unfolded forms of the protein, m_N and m_U are the slopes for the dependence of the spectroscopic properties X_N and X_U on denaturant concentration, ΔG_{H_2O} is the apparent free energy difference between the folded and the unfolded forms of the protein extrapolated to [D] = 0, m_G is the slope describing the dependence of ΔG_{H_2O} on [D] (assuming a linear relationship between the natural log of the equilibrium constant and denaturant concentration), R is the ideal gas constant, and T is the temperature. The midpoint of the transition can be calculated by dividing ΔG_{H_2O} by m_G, but the propagation of error for these two terms caused unrealistically large standard deviations for the midpoint of denaturation. Instead, the midpoint of the transition was determined by substituting ΔG_{H_2O}/midpoint for m_G in Equation (2). The criteria of Mannervik[28] and Motulsky and Ransas[29] were used to assess the goodness of the fit to the various models. When the standard error of a parameter exceeded the value of that parameter determined by fitting, the parameter was eliminated from the above equation, and the fit repeated. This process was continued until all the remaining terms were significant.

Kinetic Analysis

Unfolding and refolding kinetics were monitored by stopped-flow circular dichroism. A Jasco J-710 spectropolarimeter in conjunction with a RX1000 stopped-flow apparatus (Applied Photophysics) was used to monitor intensity changes at 218 nm (2 nm bandpass).[15] Five parts of denaturant solution were mixed with one part protein solution. Final protein concentrations were 32–33 μM. The dead time of mixing was determined to be 15–30 ms.[15] The instrumental time constant was 8 ms for IFABP and CRBP II and 32 ms for CRABP I. Since CRABP I folds and unfolds much slower than the other proteins, a longer time constant was used to improve the signal to noise. A maximum of 2,000 data points was collected for each kinetic transition with 5–7 consecutive traces averaged. Due to instrument limitations, refolding reactions longer than 100 seconds could not be performed with this apparatus. Additional refolding experiments for CRABP I were performed on an AVIV 62DS spectropolarimeter with a Biologic SFM-3 stopped-flow module. The dead time for this instrument has been determined to be 5 ms.[30] CRABP I was diluted 1:10 with denaturant solutions to a final protein concentration of 13 μM. Five to forty kinetic traces (1,000 data points per trace) were averaged.

Unfolding and refolding kinetics were monitored by fluorescence using an Applied Photophysics DX-17MV stopped-flow spectrophotometer. For both CRABP I and IFABP fluorescence measurements were made at 25°C by exciting at 290 nm (2.3 nm bandpass) via a 0.2-cm pathlength and monitoring the emission intensity above 305 nm at 90° with a WG305 Schott glass filter (Oriel). The close similarity in intensity for the native and unfolded forms of CRBP II led to little if any signal change when the total intensity change above 305 nm was observed. For CRBP II excitation was at 290 nm (9.3 nm bandpass) and an emission wavelength of 327 nm (18.6 nm bandpass) was used. For both unfolding and refolding experiments, 2.5 ml and 0.5 ml drive syringes were employed to mix five parts denaturant solution (0–9 M urea) with one part protein solution. Final protein concentrations were 17 μM IFABP, 11 μM CRABP I, and 33 μM CRBP II. For each urea concentration, five to seven consecutive traces were averaged. The dead time at this mixing ratio was determined to be 5–10 ms, depending on the denaturant concentration.[15]

The program supplied by Applied Photophysics was used to determine the nonlinear least-squares fits of the fluorescent kinetic data to the equation:

$$A(t) = \Sigma A_i \exp(-k_i t) + A_\infty \quad (3)$$

where A(t) is the amplitude of the change at time t, A_∞ is the amplitude at infinite time, A_i is the amplitude at zero time of phase i, and k_i is the rate of phase

```
Structure      <====ßA====> <===αI==>  <===αII===><===ßB===>   <==ßC==>  <===ßD==>
IFABP      ---AFDGTWKVYRNENYEKFMEKMGINVVKRKLGAHDNLK--LTITQEGNKFTVKESSNFRNIDVVFELGVD
CRBPII     MTKDQNGTWEMESNENFEGYMKALDIDFATRKIAVRLTQT--KIIVQDGDNFKTKTNSTFRNYDLDFTVGVE
CRABPI     -MPNFAGTWKMRSSENFDELLKALGVNAMLRKVAVAAASKPHVEIRQDGDQFYIKTSTTVRTTEINFKVGEG
Homology         *** .   **..  .  . .    **.          * *.*  *  *  .. *. .. * .*

Structure  <==ßE==>   <===ßF==>   <===ßG===>   <===ßH===>  <==ßI==>  <===ßJ===>
IFABP      FAYSL--ADGTELTGTWTMEG-NKLVGKFKR-VDNGKELIAVREISGNELIQTYTYEGVEAKRIFKKE
CRBPII     FDEHTKGLDGRNVKTLVTWEG-NTLVCVQ---KGEKENRGWKQWVEGDKLYLELTCGDQVCRQVFKKK
CRABPI     FEEET--VDGRKCRSLPTWENENKIHCTQTLLEGDGPKTYWTRELANDELILTFGADDVVCTRIYVRE
Homology   *       **       * *. * .                  . . .  *          . ... .
```

Fig. 2. Clustal W multiple sequence alignment of rat IFABP, rat CRBP II, and mouse CRABP I showing the identity (16%) and similarity (33%) among the three sequences. The few amino acids which are highly conserved throughout the entire iLBP family are boxed.

i. The CD kinetic data was fit to mono- and biexponential decay equations using KaleidaGraph. Additional phases were added to the equation until no significant improvement in the residual sum of the squares was observed. Goodness-of-fit was assessed by the same criteria used for the equilibrium analysis.

RESULTS

Structure and Sequence Comparison

The structures of CRABP I, CRBP II, and IFABP are strikingly similar (Fig. 1), despite having significant differences in their amino acid sequence (Fig. 2). Greater than 80% of the backbone atoms of each protein could be superimposed. The pairwise root mean square deviation (RMSD) for the homologous alpha carbons were 1.58 Å, 1.47 Å, and 1.59 Å, for IFABP and CRABP I, CRBP II and CRABP I, and IFABP and CRBP II, respectively. For the sake of comparison, the same protein in two different crystal lattice positions may have an RMSD of 0.1 to 0.35 Å.[6] The pairwise RMSD between the coordinates for the alpha carbons from the X-ray and NMR-derived structures of IFABP was 2.3 Å.[31]

The overall sequence alignment of the three proteins showed only 16% sequence identity and 33% similarity (Fig. 2). The similarities for the pairwise alignments were 36% identical and 60% similar for CRABP I and CRBP II, 28% identical and 53% similar for IFABP and CRABP I, and 31% identical and 48% similar for IFABP and CRBP II.

Spectral Comparisons

The far-UV circular dichroism spectra for the native and denatured states of the proteins are shown in Figure 3A. The minimum for the native proteins was approximately 216 nm, typical for β-sheet proteins.[32] Although the shapes of the spectra were similar, there were significant intensity differences. The mean residue ellipticity at 216 nm for CRBP II was nearly twice as great as that of CRABP I and IFABP. Another difference in the ellipticity of these proteins was observed between 228 and 238 nm, where both CRABP I and IFABP showed a small negative signal but CRBP II had none. The CD spectra for CRABP I and CRBP II were similar in shape and intensity to those previously

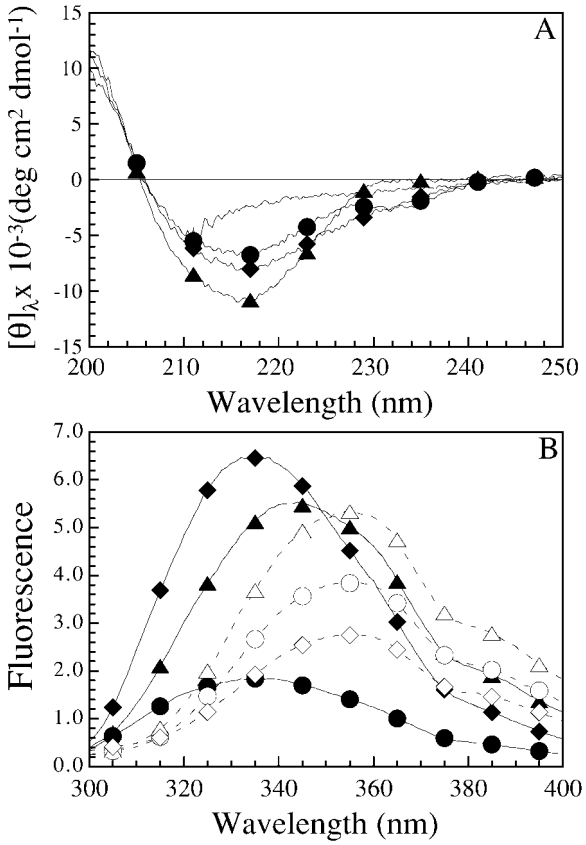

Fig. 3. The far-UV CD spectra (**A**) and fluorescence emission spectra (**B**) of the native (0 M urea) and denatured (8.2 M urea) states of CRABP I (●, ○), CRBP II (▲, △), and IFABP (◆, ◇) in 25 mM $NaPO_4$, 75 mM NaCl, 0.1 mM EDTA, and 0.1 mM DTT, pH 8.0. The protein concentrations for CD and fluorescence were 7.5 μM and 0.75 μM, respectively. The far-UV CD spectra of the denatured states were identical for all proteins and are represented by the trace without symbols. The excitation wavelength for the fluorescence emission spectra was 290 nm (2 nm bandpass), with the denatured states indicated by a dotted lines. The symbols are used to aid in identifying spectra. Data were collected every 1 nm for fluorescence and every 0.2 nm for CD.

reported.[17–19] The CD spectra of the unfolded proteins were identical.

The fluorescence spectra of the native proteins differed as well (Fig. 3B). Both IFABP and CRABP I had the same wavelength of maximal emission (334

nm), but IFABP exhibited a four-fold greater intensity, despite having only two tryptophans compared to the three of CRABP I. CRBP II, which has four tryptophans, had a maximal wavelength of emission of 344 nm. The wavelength of maximal emission for all of the denatured proteins was 354 nm. The fluorescence intensity of the unfolded state was directly proportional to the number of tryptophan residues in the sequence. The shoulder at 390 nm in these spectra is due to a monochromater artifact.

Equilibrium Unfolding

All of these proteins exhibited a completely reversible transition during urea denaturation as monitored by both CD and fluorescence at equilibrium (Fig. 4). The data by both optical methods were best fit to a two-state model for all of the proteins. Table I summarizes the results of these fits. The proteins had free energies (linearly extrapolated to 0 M urea, ΔG_{H_2O}), ranging between 5–9 kcal/mol, by both CD and fluorescence (Table I). The ΔG_{H_2O} and midpoint for urea denaturation of CRBP II were higher than those of CRABP I and IFABP. The midpoints of denaturation were identical by both optical methods.

Kinetics of Folding and Unfolding

Unfolding and refolding kinetics for CRABP I and CRBP II were monitored by stopped-flow CD and fluorescence. In order to determine the expected amplitudes for each change in denaturant concentration, the initial and final fluorescence and CD intensities were used to construct equilibrium unfolding curves. Examples are shown in Figure 5. The ΔG_{H_2O} and midpoints calculated from these data were similar to those derived from the equilibrium measurements (Table I). The fluorescence kinetic rates and amplitudes were not dependent on protein concentration (2–40 μM, data not shown). Thus, protein aggregation is not a likely explanation for the presence of multiple phases during folding and unfolding.[33]

Unfolding kinetics

All of the expected fluorescence amplitude change was observed during unfolding (Fig. 5). An example of the unfolding of CRABP I as monitored by fluorescence is shown in Figure 6. The unfolding of these proteins was a multiphasic process. The fit of a biphasic exponential equation was clearly superior to the fits to either a single exponential equation or to a single exponential equation with an additional linear loss in intensity due to photobleaching (Fig. 6). Approximately 90% of the fluorescence amplitude change occurred at the slower of the two observed rates for CRABP I. The faster phase accounted for only 10% of the total amplitude. The unfolding of IFABP and CRBP II were also biphasic processes by fluorescence. However, the majority of the fluorescence amplitude change (80–90%) occurred during the faster phase for these two proteins, with the slower rate accounting for 10–20% of the total amplitude. The dependence of the rates of unfolding on denaturant concentration are shown in Figure 7.

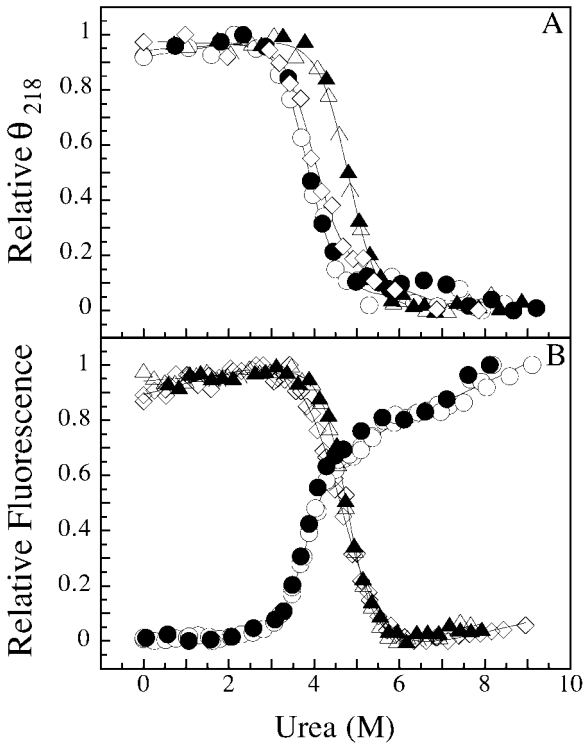

Fig. 4. Representative plots of the urea-induced unfolding at equilibrium of CRABP I (○), CRBP II (△), and IFABP (◇) monitored by CD (**A**) and fluorescence (**B**) in 25 mM $NaPO_4$, 75 mM NaCl, 0.1 mM EDTA, 0.1 mM DTT, pH 8.0. The loss of secondary structure was monitored at 218 nm. The fluorescence emission was monitored for CRABP I, CRBP II, and IFABP at 355 nm, 327 nm, and 340 nm, respectively, upon excitation at 290 nm. Protein concentrations for far-UV CD and fluorescence were 7 μM and 0.7 μM, respectively. Reversibility is shown with filled symbols.

The entire expected amplitude was observed by CD during unfolding, as well. In contrast to fluorescence, the CD unfolding kinetics were best fit to a monoexponential process for each protein. The rate observed by CD corresponded to the faster of the two rates observed by fluorescence for IFABP and CRBP II (Fig. 7). The rate observed by CD for CRABP I corresponded to the slower of the two rates observed by fluorescence for this protein (Fig. 7). The rates for unfolding were significantly different for each protein. IFABP unfolded four- to five-fold faster than CRBP II and 30- to 100-fold faster than CRABP I (Fig. 7).

Refolding kinetics

During refolding, burst phases were observed by fluorescence and CD for all of these proteins. For IFABP and CRBP II, the burst phase resulted in a state with less fluorescence than expected for the unfolded protein. In the case of CRABP I, the observed fluorescence amplitude exceeded the expected value (Fig. 5). The amplitude of the burst phase increased at lower final concentrations of

TABLE I. Thermodynamic Parameters for the Equilibrium Unfolding of CRABP I, CRBP II, and IFABP†

	ΔG_{H_2O} (kcal/mol)	m_G (kcal/(mol * M)	Midpoint (M)	ΔASA (Å^2)
CRABP I				
θ_{218}	6.39 ± 0.59	−1.69 ± 0.15	3.78 ± 0.04	16,686
θSF_{218}	5.12 ± 1.47	−1.35 ± 0.37	3.78 ± 0.14	
F_{355}	6.62 ± 0.34	−1.76 ± 0.09	3.76 ± 0.02	
$FSF_{>305}$	5.27 ± 1.02	−1.46 ± 0.28	3.61 ± 0.09	
CRBP II				
θ_{218}	8.19 ± 0.40	−1.70 ± 0.09	4.83 ± 0.02	16,713
θSF_{218}	7.05 ± 1.53	−1.47 ± 0.31	4.81 ± 0.09	
F_{327}	8.43 ± 0.29	−1.76 ± 0.06	4.78 ± 0.01	
FSF_{327}	9.40 ± 0.61	−1.99 ± 0.13	4.73 ± 0.03	
IFABP				
θ_{218}	4.79 ± 0.30	−1.16 ± 0.07	4.12 ± 0.03	16,140
θSF_{218}	5.11 ± 0.59	−1.27 ± 0.15	4.03 ± 0.06	
F_{340}	5.07 ± 0.35	−1.21 ± 0.08	4.20 ± 0.04	
$FSF_{>305}$	5.89 ± 0.36	−1.43 ± 0.09	4.13 ± 0.03	

†θ, ellipticity; F, fluorescence; SF, stopped flow. Subscript indicates wavelength. ΔG_{H_2O}, m_G, midpoint, and ΔASA were determined as described in Materials and Methods.

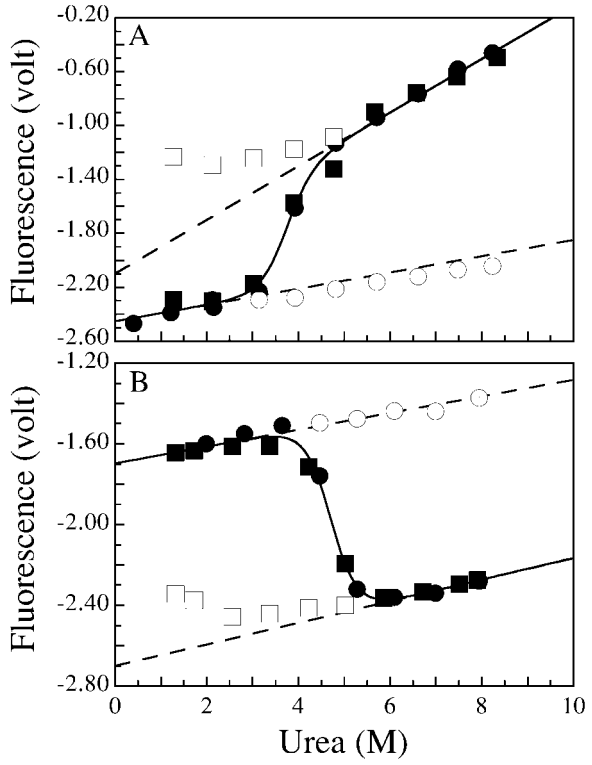

Fig. 5. The fluorescence equilibrium endpoints obtained from unfolding (●) and refolding (■) stopped flow experiments, illustrating the refolding burst phase observed for CRABP I (**A**) and CRBP II (**B**). Open symbols represent the initial fluorescence signal at the start of the kinetic transition. Dotted lines indicate the expected initial fluorescence signal based on extrapolated native and denatured baselines.

denaturant for each protein. At concentrations of denaturant near the equilibrium unfolding transition, the magnitude of the fluorescence burst phase was small or absent (Fig. 5). At the lowest final urea concentration examined (1 M), at least 60% of the expected CD amplitude change occurred in the dead time of mixing. As the final concentration of denaturant increased, the amplitude of the burst phase by CD decreased. At 3 M final urea concentration, 45%, 30%, and 40% of the expected CD amplitude change occurred in the dead time of mixing for IFABP, CRABP I, and CRBP II, respectively.

The observed recovery of fluorescence during refolding of IFABP, CRBP II, and CRABP I were monophasic, biphasic, and triphasic, respectively. Triphasic refolding was previously observed for CRABP I at a single final denaturant concentration.[19] An example of a typical refolding transition for CRBP II is shown in Figure 8. The fastest phase for both CRABP I and CRBP II accounted for approximately 65% and 85%, respectively, of the total observed amplitude. A monophasic recovery of the remaining CD signal was detected for all of the proteins by CD (Fig. 7). In each case, the observed CD rate was the same as the fastest rate observed by fluorescence.

Dramatic differences in the overall refolding rates were observed for these proteins (Fig. 7). At a final urea concentration of 1 M, IFABP had a refolding rate 20-fold slower than CRBP II. CRABP I refolded five-fold slower than IFABP (100-fold slower than CRBP II). Differences in the refolding rate of CRABP I and IFABP were amplified as the final urea concentration was increased. At 4 M urea, the rate of refolding of CRABP I was 100-fold slower than that of IFABP. In contrast, the rate of refolding of CRBP II converged with that of IFABP as the final urea concentration increased (Fig. 7).

DISCUSSION

Several investigators have compared the folding mechanism of structurally homologous proteins from different species. However, these proteins had either

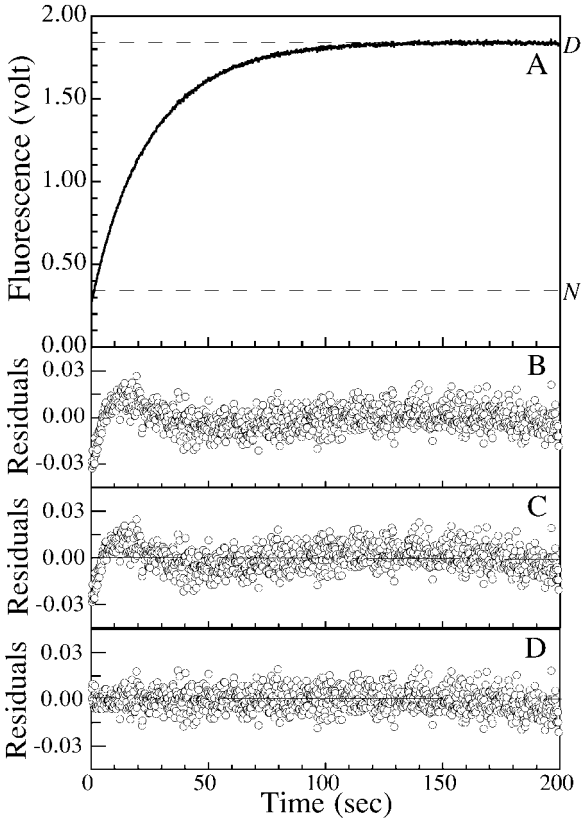

Fig. 6. The unfolding kinetic transition of CRABP I (**A**), and the residuals of a (**B**) single, (**C**) single with steady state, and (**D**) double exponential fit. The extrapolated fluorescence of the native (N) state in 8 M urea and the denatured (D) state are indicated by the dashed lines and demonstrate that all of the expected amplitude is present (within error). The protein concentration was 11 μM and the fluorescence unfolding transition was initiated by rapid dilution (1:6) of the protein in 2 M urea to a final urea concentration of 8.2 M using the following buffer: 25 mM $NaPO_4$, 75 mM NaCl, 0.1 mM EDTA, 0.1 mM DTT pH 8.0.

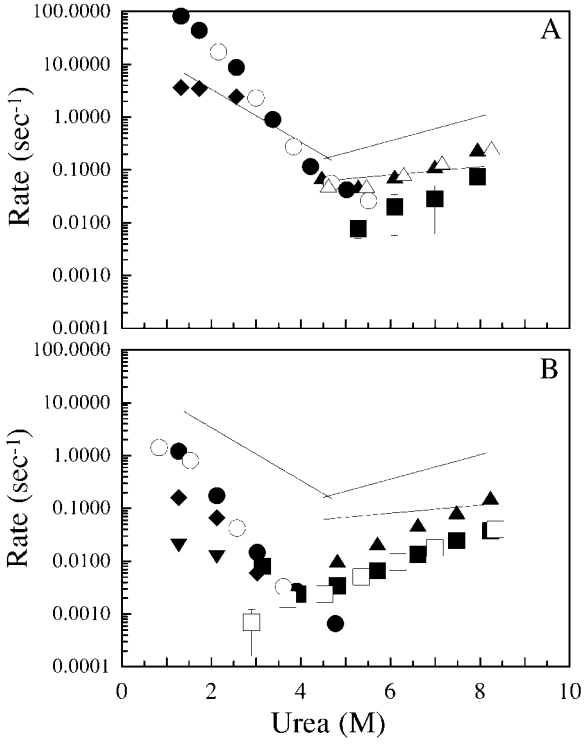

Fig. 7. The dependence of the rates of unfolding and refolding on urea for CRBP II (**A**) and CRABP I (**B**), monitored by stopped-flow CD (open symbols) and stopped-flow fluorescence (filled symbols). Error bars fall within the symbol, unless shown. The kinetic phases for IFABP[15] are plotted as straight lines, for comparison. The loss and gain of secondary structure was monitored at 218 nm with one detectable phase for all of the proteins (open symbols). Tryptophan fluorescence emission was monitored at 327 nm for CRBP II and at >305 nm for CRABP I and IFABP. Protein concentrations were 33 μM (IFABP and CRBP II) and 32 μM (CRABP I) for CD, and 17 μM (IFABP), 33 μM (CRBP II), and 11 μM (CRABP I) for fluorescence. Two fluorescence unfolding phases were detected for all of the proteins (▲ and ■). Two and three fluorescence refolding phases were detected for CRBP II (● and ◆) and CRABP I (●, ◆, and ▼), respectively. The following buffer was used for all kinetic assays: 25 mM $NaPO_4$, 75 mM NaCl, 0.1 mM EDTA, pH 8.0 with 0.1 mM DTT added to CRABP I and CRBP II reaction assays only.

disulfide bonds or much higher sequence identities within their families than the iLBPs: 85% identity for the alpha subunit of *E. coli* and *S. typhimurium* tryptophan synthase,[34] 60% identity for hen and human lysozyme,[35] 44% identity for rat and yeast acyl-coenzyme A-binding protein,[36] 65% identity for mammalian RNases,[37] and 33% identity for bovine pancreatic trypsin inhibitor and proteins I and K from black mamba venom (disulfide containing proteins).[38] Studies on these systems suggested that the folding mechanism of structurally homologous proteins was conserved, since similar kinetics of the folding process were observed. The low sequence identity for the iLBP family implied a higher degree of allowed amino acid substitutions for this fold. This degeneracy resulted in different folding and unfolding mechanisms for these proteins.

The ribbon diagrams in Figure 1 show the high degree of similarity between these structures. The backbone structure is highly conserved with the core β-sheet regions intact. Three regions in the structure showed the greatest variation. The first occurs in the turn from helix II to strand B, where CRABP I has a two amino acid insertion compared to the other two proteins. The second dissimilar region is the location of strand E relative to the rest of the upper β-sheet. Strand E is indirectly hydrogen bonded to strand D via water molecules, and this relayed hydrogen bond network leads to an unusually large gap between strands D and E. Finally, the lengths of strands G and H are different for these proteins, leading to a poor overlap of structure in this region. These regions show the greatest deviation between the X-ray and NMR derived structures of IFABP.[31]

Spectral Characterization

Given the close conservation in structure for these proteins, the large differences in the far-UV CD spectra of their native states was unexpected. CRBP

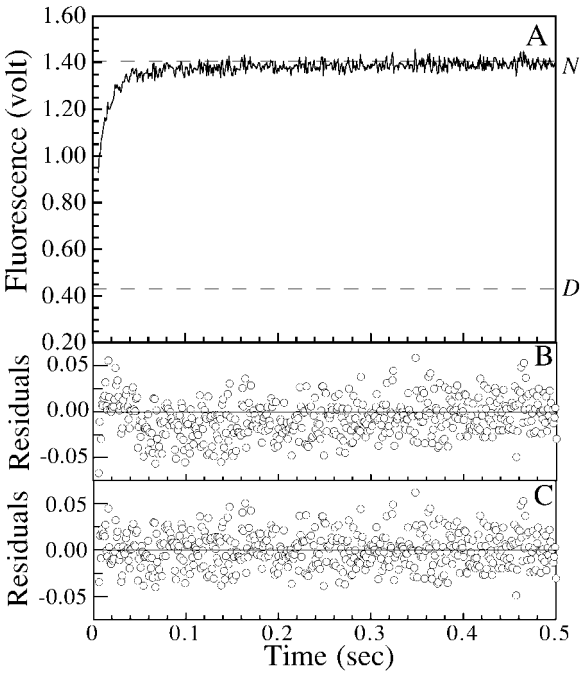

Fig. 8. The refolding kinetic transition of CRBP II (**A**), and the residuals for (**B**) a single with steady state, and (**C**) a double exponential fit with steady state. The protein concentration was 33 μM and the fluorescence refolding transition was initiated by rapid dilution (1:6) of the protein in 8 M urea to a final urea concentration of 1.3 M using the following buffer: 25 mM $NaPO_4$, 75 mM NaCl, 0.1 mM EDTA, 0.1 mM DTT pH 8.0.

II had nearly twice the diagnostic β-sheet CD signal around 216 nm as the other proteins, emphasizing the difficulties associated with predicting secondary structure from the CD spectra of β-sheet proteins.[32,39] The spectrum for CRBP II also differed from the other spectra between 228 nm and 238 nm. Both CRABP I and IFABP showed a small negative signal over this wavelength range, but no signal was detected for CRBP II. These intensity differences were probably due to the contribution of aromatic residues to the far-UV CD signal, as shown for carbonic anhydrase[40] and barnase.[41] Mutations of W87 and W109 (W87F, W109F) of CRABP I altered the CD signal around 228 nm, suggesting that these residues are involved in the CD spectral differences.[19] Other aromatic residues may contribute as well. The CD spectra of the unfolded proteins were identical, suggesting that the proteins were equally unfolded by 8 M urea.

The wavelength of maximal tryptophan fluorescence emission provides a qualitative measure of the polarity of the local environments.[42] Lower wavelengths of maximal emission correspond to more hydrophobic environments. The emission spectra of CRBP II was red-shifted 10 nm relative to the other proteins. The structures of CRBP II and CRABP I showed that the three tryptophans of CRABP I (W7, W87, W109) have identical positions to three of the four tryptophans of CRBP II (W8, W88, W106). The additional tryptophan of CRBP II (W109) is directed outward into solvent. The solvent-accessible surface area of this tryptophan was much greater than the other tryptophan residues in CRBP II, and mutation of this residue to phenylalanine resulted in a protein whose maximal wavelength of emission was similar to that of CRABP I.[43] These proteins had the same wavelength of maximal emission in the urea denatured state, indicating that the environments of the tryptophans in the unfolded states were similar. The fluorescence intensity in the unfolded state correlated directly with the number of tryptophan residues in each protein (four for CRBP II, three for CRABP I, and two for IFABP).

Equilibrium Analysis

Each of these proteins exhibited a reversible two-state, unfolding transition in urea by both CD and fluorescence, suggesting that no significant concentrations of intermediates were present at equilibrium.[44] The ΔG_{H_2O} values obtained from the two-state fit ranged from 5–9 kcal/mol, typical for small globular proteins.[45] The sequence changes among these proteins apparently caused the observed differences in stability, with CRBP II being the most stable and IFABP being the least stable (Table I). CRBP II and CRABP I had similar dependencies of ΔG_{H_2O} on denaturant concentration (m_G), whereas IFABP had a lower value. The change in solvent-exposed surface area during unfolding (ΔASA) has been shown to be correllated with m_G,[46] but there were very small differences in the calculated ΔASA for these three proteins (Table I). As such, the variation in m_G among these proteins was not due to differences in the calculated change in solvent-exposed surface area for these sequences. Although no differences in the structure of the unfolded states of these proteins were observed by circular dichroism or fluorescence, there might still be differences in the organization of the unfolded states of these proteins, as suggested for mutants of staphylococcal nuclease,[47] causing the observed differences in m_G.

Unfolding Kinetics

The unfolding kinetics for these proteins were biphasic, but differed with respect to their rates and amount of secondary structure change associated with each phase. It is unusual for the unfolding of small globular proteins to be multiphasic.[48] Two paths for unfolding were found during the unfolding of barnase, leading to very complex unfolding kinetics.[49] There is no need to invoke multiple paths for the unfolding of these proteins. A simple path with a single intermediate can explain the observations for each protein. The discussion of the kinetics of folding and unfolding is based on the classical model for protein folding, in order to provide a framework to compare and contrast these systems.

CRABP I showed two phases during the unfolding process by fluorescence. The slower phase was ob-

served by CD; but the faster phase, which accounted for about 10% of the expected fluorescence amplitude change, was not observed by CD. Any secondary structure change associated with this phase must have been small, or it would have been detected. The simplest model that explained these results required an intermediate on the unfolding pathway:

$$N \Rightarrow I \Rightarrow U.$$

This intermediate appears to be a molten globule, which is defined here as a protein with native-like secondary structure but perturbed and fluctuating tertiary contacts compared to the native state.[50]

IFABP and CRBP II also showed two fluorescence phases during unfolding. However, unlike CRABP I, the faster of the two phases observed by fluorescence corresponded to the observed CD transition. The simplest model for the unfolding of IFABP and CRBP II has the same form as that of CRABP I. However, the spectral properties of the observed intermediates for IFABP and CRBP II were different from those of CRABP I. The lack of a CD signal change associated with the second slower fluorescence rate suggests that the intermediate present during the unfolding of IFABP and CRBP II had little if any secondary structure associated with it. Thus, the intermediate observed during the unfolding of these two proteins was not a molten globule.

Refolding Kinetics

The refolding kinetics were more difficult to interpret, due to the presence of a significant burst phase for each of the proteins. The burst phase detected by CD for these proteins was always followed by a monophasic recovery of the remainder of the native state CD signal. The burst phases by fluorescence were followed by a monophasic, biphasic, and triphasic recovery of native state fluorescence for IFABP, CRBP II, and CRABP I, respectively. The nature of this initial burst state and its importance to the further folding of any protein showing this behavior is not well understood. In some cases, these states are considered to be similar to the molten globules formed at low pH and high ionic strength by many proteins.[50] These molten globules have native-like topology and secondary structure, but the compact tertiary structure is not present. IFABP does form a molten-globule like state at low pH, but neither the fluorescence nor CD spectrum of that state are similar to the burst phase spectra described here.[51]

The initial state formed during the folding of these proteins might be a collapsed, unfolded form.[52] The linear extrapolation of the optical signals in the unfolded state to low concentrations of denaturant (as shown in Figure 5) was shown to be incorrect for some proteins, because low denaturant concentrations in water are poor solvents for many extended peptide chain sequences. Hydrophobic forces would cause a rapid compaction of these extended chains. This process results in a state that is still denatured but has different spectral properties from that of the extended chain.[52] The optical changes that occurred during the burst phase for these proteins may not be the result of the formation of native-like structures, but may be due to more random hydrophobic interactions. In the case of IFABP, the initial observed state has considerable secondary structure by CD criteria, but few if any of the hydrogen bonds that are responsible for this CD signal are protected from exchange with solvent (data not shown). A similar lack of protection from exchange of a burst-phase hydrogen bond network detected by CD was shown for CRABP I,[53] although the quench buffer pH was unusual for such studies. As such, these initial states during the folding of the iLBPs may be compact denatured states, rather than molten globules with native-like structures.

The simplest models describing the observed changes during folding of these proteins were:

$$\text{IFABP: BURST} \Rightarrow N$$

$$\text{CRBP II: BURST} \Rightarrow I \Rightarrow N$$

$$\text{CRABP I: BURST} \Rightarrow I_1 \Rightarrow I_2 \Rightarrow N$$

The fastest refolding rates observed by fluorescence corresponded to the single observed rate by CD for all of these proteins. Thus, the changes in tertiary structure associated with the slower fluorescence rates during the folding of CRBP II and CRABP I did not correspond to further changes in the overall secondary structure of the proteins. Local rearrangements involving one or more of the tryptophans of CRABP I and CRBP II were required to reach the final native state after secondary structure was formed. Three of the four tryptophans of CRBP II have analogous structural positions in CRABP I. However, two intermediates were observed during the folding of CRABP I, while CRBP II had only one. The mechanism of refolding of the iLBPs were more similar than their unfolding, since all of the secondary structure and most if not all of the native state fluorescence was recovered in the first phase after the initial burst. However, there were adjustments in the tertiary structure for CRBP II and CRABP I after secondary structure had been formed.

Relative Rates of Folding and Unfolding

The overall rates of folding and unfolding of CRABP I were about 1,000-fold slower than those of CRBP II and IFABP, suggesting that the transition state barrier between the folded and unfolded states were higher for CRABP I under all solvent conditions. Structurally, there are no obvious reasons why these kinetic transitions for CRABP I were so much slower. Proline isomerization has been associated with the slow phases during the refolding of many proteins (reviewed in reference 54), and was reported to be

associated with the slow phases of refolding of CRABP I[53]—although no data was shown. CRABP I had the slowest refolding rate of all of these proteins, and is the only one of these three proteins with proline residues. All four prolines of CRABP I are in the trans configuration in the native state, which is also the favored conformation in the unfolded state.[54] Preliminary manual mixing double-jump experiments were performed in order to determine if proline isomerization was involved in the slow refolding steps.[54] CRABP I was unfolded for various lengths of time and then rapidly returned to native conditions (data not shown). In these experiments, the amplitudes and rates of the slow phases did not change significantly with increasing incubation time (2 minutes to 2 hours) under denaturing conditions. Given the slow rate of unfolding of CRABP I, these experiments did not conclusively prove that proline isomerization was not involved in the slow refolding phases, but it seems unlikely. Further, proline isomerization alone cannot explain the slow unfolding of CRABP I, since the prolines were in a single conformation in the native structure.

Hypotheses on the Kinetic Differences

The observed folding and unfolding kinetics were very different for these structurally related proteins. One possible explanation for these observations is based on the structural locations of the residues that are observed by fluorescence. The sequence conservation of the tryptophans in these proteins is low, with only one tryptophan site (W6 in IFABP) common to these proteins. IFABP and CRBP II have tryptophans in unique structural locations compared to the other proteins (IFABP: W82; CRBP II: W109; Fig. 1). As such, a tryptophan at either of these structural locations may be required to detect the intermediate that lacks secondary structure during the unfolding of these two proteins. A mutant of IFABP that lacked W82 (W82Y) did not show any intermediates during unfolding (data not shown), suggesting that the location of the probe for intermediate formation was important for detection. However, a mutant CRBP II (W109F), which has tryptophans in the same structural locations as CRABP I, had biphasic unfolding kinetics similar to that of wild-type CRBP II (data not shown). Thus, the structural location of W109 was not responsible for the differences in the kinetic mechanism of unfolding for CRBP II and CRABP I.

Further, this hypothesis does not explain why an intermediate with spectral properties similar to those observed for CRABP I (native-like secondary structure, perturbed fluorescence) was not observed during the unfolding of CRBP II. CRBP II has tryptophans at all of the tryptophan sites in CRABP I. As such, an intermediate with similar spectral properties should be observed if the same unfolding pathway was being followed. Although the local sequence context and the structural locations of the tryptophans in these proteins may be important to completely elucidate all the folding path for an individual protein, the differences in tryptophan locations in these proteins were not sufficient to explain why the folding and unfolding kinetics of these proteins were so different.

A second hypothesis for these kinetic differences was dependent on the overall energetics of the unfolding process. Consider the simplified energy diagram for the unfolding of homologous proteins shown in Figure 9. An intermediate state would accumulate during the unfolding of one of these two proteins. However, the stability of the intermediate for the second protein is not sufficient for it to accumulate. As such, although this second protein passes through the same state during unfolding, no signal would be detected. This explanation is a simplified, one-dimensional version of the landscape model for protein folding, since all of these proteins are passing through the same intermediate states even if they are not accumulated. The unfolding of these proteins is being examined at other pHs and temperatures, since changes in solution conditions can change the energetics of the unfolding process, and thus the observed path. Lowering the temperature to 8°C resulted in the loss of an intermediate that was detected during folding at 25°C for ubiquitin.[55] This interpretation could explain the differences observed during refolding, as well.

Finally, it may be that the unfolding and folding pathways for these proteins are truly different from each other. In this model, there are significant differences in stability of different regions in the native structure of these proteins such that completely different intermediates are detected during unfolding, in spite of the initial similarity in structure. Similarly, there may be different initiating sites and/or preferred paths for the folding of these proteins because of their sequence differences. These results support the theory that individual protein molecules can follow different paths to the native state over a complicated energy landscape, as shown for the folding of model proteins on a lattice.[1]

Speculation on the Structures of the Observed Intermediates

Although we have outlined hypotheses for the appearance of different intermediate states during the folding and unfolding of these proteins, it has been difficult to associate these models with structures. Careful examination of the native structures of these proteins showed no obvious structural or sequence features that were responsible for the observed differences. Some progress has been made in understanding which residues participate in intermediate structures during the folding and unfolding of IFABP, primarily by site-directed mutagenesis. Folding studies at equilibrium using fluorine NMR and 6-fluorotryptophan-labeled IFABP have shown

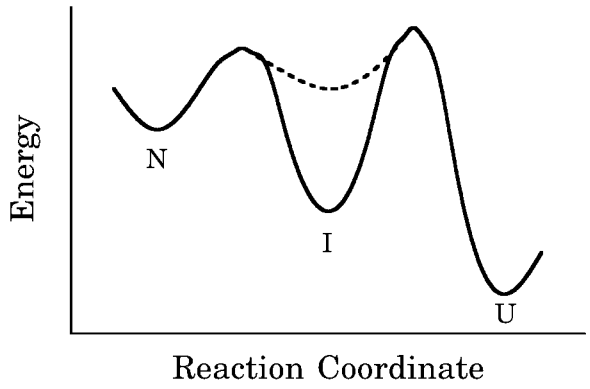

Fig. 9. Simplified energy diagram for the folding of two homologous proteins. The solid line represents a protein that passes through a stable intermediate state during folding. The dashed line represents the folding of a homologous protein for which the intermediate state is not sufficiently stable to accumulate, and thus is not detected, even though it has a similar structure.

that tryptophan-82 participated in an intermediate structure at equilibrium that lacks secondary structure, while tryptophan-6 does not.[9] The unfolding of a mutant IFABP (W82Y) was monophasic with identical rates by both CD and fluorescence (data not shown), supporting the hypothesis that some structure in the vicinity of W82 was the last part of the protein to unfold. The hydrophobic cluster surrounding W82 in the crystal structure of IFABP is present in the other proteins, and may act as a common initiating site for folding. Studies of the refolding of CRABP I have led to a hypothesis that the α-helices may act as initiating sites for folding.[18] However, the α-helices of IFABP can be deleted without changing the observed unfolding and refolding paths.[14] As such, it appears unlikely that the α-helices are important to the folding mechanism of IFABP. Finally, mutations in the D–E turn (the turn between the two strands with the unusually broad intrastrand spacing in Figure 1) greatly increased the rate of folding of IFABP, although there was a decrease in the overall stability as well.[16] Changes in these structural features in the other proteins in this family may have similar effects on the kinetics of folding of those proteins.

In summary, significant differences in the number of intermediates, the spectral characteristics of those intermediates, and the overall rates of folding and unfolding were detected for IFABP, CRBP II, and CRABP I. As such, proteins with very similar structures may not necessarily follow the same folding and unfolding paths, supporting the hypothesis that different sequences may have different energetic paths to the same final state.

ACKNOWLEDGMENTS

We thank the National Science Foundation for financial support (MCB 94-05282) and Drs. C.R. Matthews, M. Fried, C. Frieden, E. DiCera, and D. Cistola for useful discussions of these data. We thank the laboratory of Dr. C.R. Matthews for assistance in stopped-flow CD data collection.

NOTE ADDED IN PROOF

Improved experimental design has shown a weak dependence of kinetic amplitudes but not of rates for the refolding of CRABP I at protein concentrations less than 10 μM. As such, there may be a minor role for aggregation in the refolding of only this protein.

REFERENCES

1. Dill, K.A., Chan, H.S. From Levinthal to pathways to funnels. Nature Struct. Biol. 4:10–19, 1997.
2. Fersht, A.R. Nucleation mechanisms in protein folding. Curr. Opin. Struct. Biol. 7:3–9, 1997.
3. Matthews, C.R. Pathways of protein of folding. Ann. Rev. Biochem. 62:653–683, 1993.
4. Miranker, A.D., Dobson, C.M. Collapse and cooperativity in protein folding. Curr. Opin. Struct. Biol. 6:31–42, 1996.
5. Levinthal, C. Are there pathways for protein folding? J. Chim. Phys. 65:44–45, 1968.
6. Banaszak, L., Winter, N., Xu, Z., Bernlohr, D.A., Cowan, S., Jones, T.A. Lipid-binding proteins: A family of fatty acid and retinoid transport proteins. Adv. Protein Chem. 45:89–151, 1994.
7. Gordon, J.I., Sacchettini, J.C., Ropson, I.J., Frieden, C., Li, E., Rubin, D.C., Roth, K.A., Cistola, D.P. Intracellular fatty-acid-binding proteins and their genes: Useful models for diverse biological questions. Curr. Opin. Lipidol. 2:125–137, 1991.
8. Ropson, I.J., Gordon, J.I., Frieden, C. Folding of a predominantly β-structure protein: Rat intestinal fatty acid binding protein. Biochemistry 29:9591–9599, 1990.
9. Ropson, I.J., Frieden, C. Dynamic NMR spectral analysis and protein folding: Identification of a highly populated folding intermediate of rat intestinal fatty acid-binding protein by ^{19}F NMR. Proc. Natl. Acad. Sci. U.S.A. 89:7222–7226, 1992.
10. Frieden, C., Hoeltzli, S.D., Ropson, I.J. NMR and protein folding: Equilibrium and stopped-flow studies. Prot. Sci. 2:2007–2014, 1993.
11. Jiang, N., Frieden, C. Characterization of mutant proteins containing inserted cysteine residues. Biochemistry 32: 11015–11021, 1993.
12. Frieden, C., Jiang, N., Cistola, D.P. Intestinal fatty acid binding protein: Folding of fluorescein-modified proteins. Biochemistry 34:2724–2730, 1995.
13. Cistola, D.P., Kim, K., Rogl, H., Frieden, C. Fatty acid interactions with a helix-less variant of intestinal fatty acid-binding protein. Biochemistry 35:7559–7565, 1996.
14. Kim, K., Cistola, D.P., Frieden, C. Intestinal fatty acid binding protein: The structure and stability of a helix-less variant. Biochemistry 35:7553–7558, 1996.
15. Ropson, I.J., Dalessio, P.M. Fluorescence spectral changes during the folding of intestinal fatty-acid binding protein. Biochemistry 36:8594–8601, 1997.
16. Kim, K., Ramanathan, R., Frieden, C. Intestinal fatty acid binding protein: A specific residue in one turn appears to stabilize the native structure and be responsible for slow folding. Prot. Sci. 6:364–372, 1997.
17. Zhang, J., Liu, Z.P., Jones, A., Gierasch, L.M., Sambrook, J.F. Mutating the charged residues in the binding pocket of cellular retinoic acid-binding protein simultaneously reduces its binding affinity to retinoic acid and increases its thermostability. Proteins 13:87–99, 1992.
18. Liu, Z.P., Riao, J., Gierasch, L.M. Equilibrium folding studies of cellular retinoic acid binding protein, a predominantly β-sheet protein. Biochemistry 33:134–142, 1994.

19. Clark, P.L., Liu, Z.P., Zhang, J., Gierasch, L.M. Intrinsic tryptophans of CRABP I as probes of structure and folding. Prot. Sci. 5:1108–1117, 1996.
20. Sacchettini, J.C., Banaszak, L.J., Gordon, J.I. Expression of rat intestinal fatty acid binding protein in E. coli and its subsequent structural analysis: A model for studying the molecular details of fatty acid-protein interaction. Mol. Cell. Biochem. 98:81–93, 1990.
21. Norris, A.W., Cheng, L., Giguére, V., Rosenberger, M., Li, E. Measurement of subnanomolar retinoic acid binding affinities for cellular retinoic acid binding proteins by fluorometric titration. Biochim. Biophys. Acta 1209:10–18, 1994.
22. Li, E., Locke, B., Yang, N.C., Ong, D.E., Gordon, J.I. Characterization of rat cellular retinol-binding protein II expressed in *Escherichia coli*. J. Biol. Chem. 262:13773–13779, 1987.
23. Glatz, J.F.C., Veerkamp, J.H. A radiochemical procedure for the assay of fatty acid binding by proteins. Anal. Biochem. 132:89–95, 1983.
24. Pace, C.N., Vajdos, F., Fee, L., Grimsley, G., Gray, T. How to measure and predict the molar absorption coefficient of a protein. Prot. Sci. 4:2411–2423, 1995.
25. Pace, C.N. Determination and analysis of urea and guanidine hydrochloride denaturation curves. Methods Enzymol. 131:266–280, 1986.
26. Eisenhaber, F., Argos, P. Improved strategy in analytic surface calculation for molecular systems: Handling of singularities and computational efficiency. J. Comp. Chem. 14:1272–1280, 1993.
27. Santoro, M.M., Bolen, D.W. Unfolding free energy changes determined by the linear extrapolation method: Unfolding of phenylmethanesulfonyl α-chymotrypsin using different denaturants. Biochemistry 27:8063–8068, 1988.
28. Mannervik, B. Regression analysis, experimental error, and statistical criteria in the design and analysis of experiments for discrimination between rival kinetic models. Methods Enzymol 87:370–390, 1982.
29. Motulsky, H.J., Ransnas, L.A. Fitting curves to data using nonlinear regression: A practical and nonmathematical review. FASEB J. 1:365–374, 1987.
30. Mann, C.J., Matthews, C.R. Structure and stability of an early folding intermediate of *Escherichia coli* trp Aporepressor measured by far-UV stopped-flow circular dichroism and 8-anilino-1-naphthalene sulfonate binding. Biochemistry 32:5282–5290, 1993.
31. Hodsdon, M.E., Cistola, D.P. Discrete backbone disorder in the NMR solution structure of apo intestinal fatty acid-binding protein: Implications for the mechanism of ligand entry. Biochemistry 36:1450–1460, 1997.
32. Johnson, W.C. Secondary structure of proteins through circular dichroism spectroscopy. Ann. Rev. Biophys. Biophys. Chem. 17:145–166, 1988.
33. Silow, M., Oliveberg, M. Transient aggregates in protein folding are easily mistaken for folding intermediates. Proc. Natl. Acad. Sci. U.S.A. 94:6084–6086, 1997.
34. Stackhouse, T.M., Onuffer, J.J., Matthews, C.R., Ahmed, S.A., Miles, E.W. Folding of homologous proteins: Conservation of the folding mechanism of the α subunit of tryptophan synthase from *Escherichia coli, Salmonella typhimurium*, and five interspecies hybrids. Biochemistry 27:824–832, 1988.
35. Hooke, S.D., Radford, S.E., Dobson, C.M. The refolding of human lysozyme: A comparison with the structurally homologous hen lysozyme. Biochemistry 33:5867–5876, 1994.
36. Kragelund, B.B., Hojrup, P., Jensen, M.S., Schjerling, C.K., Juul, E., Knudsen, J., Poulsen, F.M. Fast and one-step folding of closely and distantly related homologous proteins of a four-helix bundle family. J. Mol. Biol. 256:187–200, 1996.
37. Lang, K., Wrba, A., Krebs, H., Schmid, F.X., Beintema, J.J. Folding kinetics of mammalian ribonucleases. FEBS Lett. 204:135–139, 1986.
38. Hollecker, M., Creighton, T.E. Evolutionary conservation and variation of protein folding pathways: Two protease inhibitor homologues from black mamba venom. J. Mol. Biol. 168:409–437, 1983.
39. Woody, R.W. Circular dichroism. Methods Enzymol. 246:34–71, 1996.
40. Borén, K., Freskgård, P.O., Carlsson, U. A comparative CD study of carbonic anhydrase isozymes with different number of tryptophans: Impact on calculation of secondary structure content. Prot. Sci. 5:2479–2484, 1996.
41. Vuilleumier, S., Sancho, J., Loewenthal, R., Fersht, A.R. Circular dichroism studies of barnase and its mutants: Characterization of the contribution of aromatic side chains. Biochemistry 32:10303–10313, 1993.
42. Permyakov, E.A. "Luminescent Spectroscopy of Proteins." Boca Raton, Florida: CRC Press, 1993.
43. Locke, B.C., MacInnis, J.M., Qian, S., Gordon, J.I., Li, E., Fleming, G.R., Yang, N.C. Fluorescence studies of rat cellular retinol binding protein II produced in *Escherichia coli:* An analysis of four tryptophan substitution mutants. Biochemistry 31:2376–2383, 1992.
44. Lumry, R., Biltonen, R., Brandts, J.F. Validity of the two-state hypothesis for conformational transitions of proteins. Biopolymers 4:917–944, 1966.
45. Privalov, P.L. Stability of proteins: Small globular proteins. Adv. Protein Chem. 33:167–241, 1979.
46. Myers, J.K., Pace, C.N., Scholtz, J.M. Denaturant m values and heat capacity changes: Relation to changes in accessible surface areas of protein unfolding. Prot. Sci. 4:2138–2148, 1995.
47. Shortle, D. Staphylococcal nuclease: A showcase of m-value effects. Adv. Protein Chem. 46:217–247, 1995.
48. Goldenberg, D.P. Genetic studies of protein stability and mechanisms of folding. Ann. Rev. Biophys. Biophys. Chem. 17:481–507, 1988.
49. Zaidi, F.N., Nath, U., Udgaonaker, J.B. Multiple intermediates and transition states during protein unfolding. Nat. Struct. Biol. 4:1016–1024, 1997.
50. Kuwajima, K. The molten globule state as a clue for understanding the folding and cooperativity of globular-protein structure. Proteins 6:87–103, 1989.
51. Dalessio, P.M., Ropson, I.J. pH dependence of the folding of intestinal fatty-acid binding protein. Arch. Biochem. Biophys., in press.
52. Sosnick, T.R., Shtilerman, M.D., Mayne, L., Englander, S.W. Ultrafast signals in protein folding and the polypeptide contracted state. Proc. Natl. Acad. Sci. U.S.A. 94:8545–8550, 1997.
53. Clark, P.L., Liu, Z.P., Rizo, J., Gierasch, L.M. Cavity formation before stable hydrogen bonding in the folding of a β-clam protein. Nat. Struct. Biol. 4:883–886, 1997.
54. Nall, B.T. Proline isomerization as a rate-limiting step. In Pain, R.H. (ed): Mechanisms of Protein Folding." New York: Oxford University Press, 1994:80–99.
55. Khorasanizadeh, S., Peters, I.D., Butt, T.R., Roder, H. Stability and folding of a tryptophan-containing mutant of ubiquitin. Biochemistry 32:7054–7063, 1993.
56. Winter, N.S., Bratt, J.M., Banaszak, L.J. Crystal structures of holo and apo-cellular retinol-binding protein II. J. Mol. Biol. 230:1247–1259, 1993.
57. Thompson, J.R., Bratt, J.M., Banaszak, L.J. Crystal structure of cellular retinoic acid binding protein 1 shows increased access to the binding cavity due to formation of an intermolecular β-sheet. J. Mol. Biol. 252:433–446, 1995.
58. Scapin, G., Gordon, J.I., Sacchettini, J.C. Refinement of the structure of recombinant rat intestinal fatty-acid binding apoprotein at 1.2 Å resolution. J. Biol. Chem. 267:4253–4269, 1992.